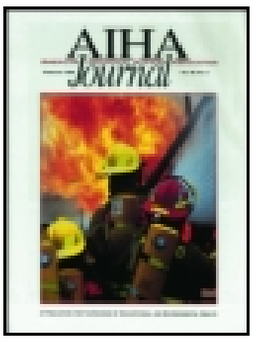

AIHAJ - American Industrial Hygiene Association

ISSN: 1529-8663 (Print) (Online) Journal homepage: https://www.tandfonline.com/loi/uaah20

Mist Generation at a Machining Center

William A. Heitbrink , James B. D'Arcy & John M. Yacher

To cite this article: William A. Heitbrink , James B. D'Arcy & John M. Yacher (2000) Mist Generation at a Machining Center, AIHAJ - American Industrial Hygiene Association, 61:1, 22-30

To link to this article: https://doi.org/10.1080/15298660008984511

Mist Generation at a Machining Center

AUTHORS
William A. Heitbrink[a]
James B. D'Arcy[b]
John M. Yacher[c]

[a]U.S. Department of Health and Human Services, Public Health Service, Centers for Disease Control and Prevention, National Institute for Occupational Safety and Health, 4676 Columbia Parkway—R5, Cincinnati, OH 45226;
[b]General Motors Research and Development Center, 30500 Mound Road, Building 1-3, Warren, MI 48090-9055;
[c]Retired

Control of occupational exposure to metalworking fluid mist generally involves enclosing the machining center and exhausting to an air cleaner that returns cleaned air to the workplace. To select an appropriate air cleaner, particle size and generation rate of the mists need to be known. Mist particle size and concentration were measured as a function of tool speed, fluid flow rate, and cutting rate at an enclosed machining center. A vertical machining center was totally enclosed and the air from this enclosure was exhausted into a duct where mist concentration and size distribution were measured using a time-of-flight aerosol spectrometer and a cascade impactor. Mist generation during the face milling of a 30 × 31-cm piece of aluminum with a 10-cm diameter face mill was studied. Machining parameters were varied as a 2 × 2 × 3 factorial experiment with these variables: coolant flow rate (18 and 44 m/sec), tool rpm (1900 and 3800 rpm), and metal removal (no removal, two teeth on face mill, and six teeth on face mill). Mist concentration increased with increasing tool speed and fluid application velocity. Whether the tool was actually removing metal did not affect the mist generation. Thus, mist generation is a function of fluid and tool motion. During a second experiment, effect of tool speed and diameter on mist generation was studied. Mist concentrations measured with the aerosol spectrometer were proportional to the 2 and 3.5 powers of the tool speed for the face mill and end mill, respectively. In both experiments the shape of the size distribution was largely unaffected by the experimental variables.

Keywords: air cleaner, metalworking fluid, mist generation

The occupational health literature contains reports linking occupational exposure to metalworking fluids (MWFs) to respiratory disease, cancer, and asthma.[1–3] Cross-shift decrements in lung function are reported for inhalable aerosol exposures larger than 0.2 mg/m³. Microbial contamination and endotoxins (debris from dead microbes) may also be responsible for adverse pulmonary health effects.[1] Some ongoing research has suggested that lifetime exposures to specific types of MWFs (straight, soluble, and synthetic) are associated with several digestive cancers. For these reasons, controlling worker exposures to MWFs is prudent. Concerns about nonmalignant respiratory disease prompted the National Institute for Occupational Safety and Health (NIOSH) to state a recommended exposure limit of 0.4 mg/m³ for thoracic particulate mass or 0.5 mg/m³ for total particulate mass.[4]

MWF mists are generated at automated, enclosed operations and at other less automated operations that cannot be tightly enclosed. The air exhausted from enclosures is processed by air cleaners and discharged back into the workplace. Selecting an appropriate air cleaner requires a knowledge of the mist's concentration, size distribution, and emission rate. If the aerosol is too small relative to the air cleaner's efficiency, mist can be dispersed throughout the plant. Consequently, a knowledge of the mist's size distribution is an important consideration in the selection of an air-cleaning device. In addition, a knowledge of factors affecting mist emissions may allow conditions to be selected to minimize mist generation and worker exposure.

To develop information needed to control occupational exposure to airborne MWFs, General Motors and NIOSH researchers jointly investigated the effect of machining parameters on MWF aerosol formation. This research was focused on identifying parameters that affected the amount and size of MWF mist that is generated during machining operations.

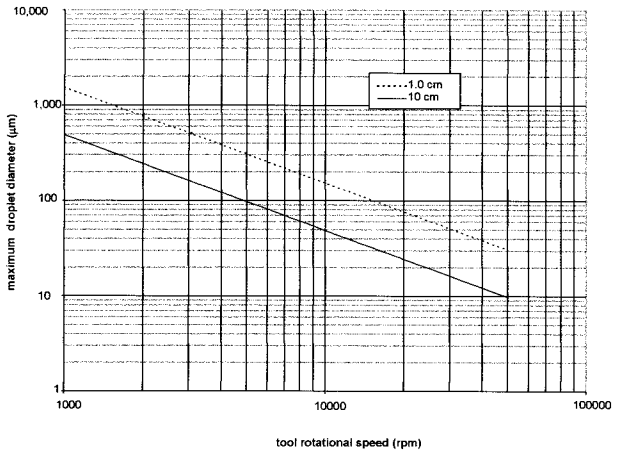

FIGURE 1. Maximum droplet diameter, after evaporation, estimated from the Weber number criteria for a fluid with a surface tension of 0.03 kg/sec² and a fluid concentration of 8%. This is the surface tension and concentration of the metalworking fluid studied in the plant.

MACHINING AND AEROSOL GENERATION

During metal removal operations such as grinding, hole drilling, boring, or face milling, MWFs are used to remove chips and heat and to provide lubrication at the tool–part interface where the tool is cutting metal from the part being machined. MWFs are usually flooded onto the part and tool at relatively low pressures, i.e., less than 50 psi. For operations such as gun drilling, the coolant is sometimes forced through the tool at relatively high pressures (e.g., 800–1200 psi) to lubricate drills and to remove chips generated during hole drilling.[5] The MWF then flows over a machine tool or a grinding wheel with rotational speeds between 1000 and 10,000 rpm. After application some of the MWF flows and falls from the points of application into a flume, which flows back to a storage tank for treatment and reuse. Also, some of the fluid is violently thrown against the walls of the enclosure. In very close proximity to the location where metal is being removed, the coolant can be heated to the point of evaporation, and this evaporated coolant could then condense to form a very small aerosol.[6] Apparently, aerosol generation during machining operations is complex. Some insights into how this generation occurs can be obtained by reviewing the literature on aerosol generation by spray atomization, splashing, foaming, and rapidly moving fluids.

Fluid Motion

As the MWF falls or flows from the point of application toward the flume or drip pan, liquid droplets can be separated from the bulk of the fluid. Mist generation by liquid jets has received some attention in the engineering science literature. When turbulent liquid jets flow from a nozzle, vortices cause small, visible liquid droplets to be emitted from the liquid surface. The formation of these droplets has been photographically observed.[7] This type of droplet generation does not necessarily involve interaction with air. High molecular weight polymers have been shown to suppress this type of mist generation. Liquid jets are said to "splatter" when spray droplets are detached from the main fluid jet or from the liquid layer that covers the target of the spray.[8,9] The amount of mist generation has been related experimentally to the root-mean-square surface vibrations of the jet and of the flow over the surface. From dimensional analysis, mist formation is a function of the jet's diameter, velocity, surface tension, viscosity, density, and distance to a target. This mist generation mechanism involves a threshold effect. For mist generation by surface vibrations, the ratio of the root-mean-square surface disturbance to the jet diameter needs to exceed 0.05 for mist generation to occur. Then mist generation increases as the magnitude of this ratio increases.

Foam or Bubble Breakup

During some MWF handling, air may be injected into the fluid causing bubbles. The breakup of bubbles can cause mist generation. MWF foaming is an abnormal condition generally controlled by the addition of defoaming agents.[10]

Rotary Atomization

During machining operations, tools or parts rotate. These rotating tools or parts, to some extent, may function as rotary atomizers that generate mist droplets. Droplet size is determined by the forces applied to atomize the fluid and the intermolecular forces opposing the break-off of droplets from the bulk fluid. Physical phenomena occurring during spraying and atomization have been the subject of much fundamental research and mathematical modeling, which have been summarized by Lefebvre.[11] The following paragraphs summarize this information.

In rotary atomizers, mist droplets are formed by direct droplet formation or by the formation of unstable ligaments that disintegrate into droplets. Centrifugal force spreads the liquid over the surface of the rotating object. At low flow rates, uniformly sized drops are formed directly on the periphery of the spinning object. As the liquid flow rate increases, ligaments, which look like strands of fluid, and sheets of fluid are emitted into the air surrounding the spinning object. Mathematical models present relationships between droplet size and the rotating object's diameter, surface features, and rotational speed; the atomization regime; and the fluid's density, surface tension, and viscosity. These models predict that particle size decreases with increasing diameter and rotational speed and with decreasing viscosity and surface tension. In these models all of the fluid applied to the part is assumed to be atomized.

Most of the models presented by Lefebvre for rotary atomization involve the liquid flow rate. In the study of machining operations, such models are difficult to use because one does not know how much fluid is actually being applied to the rotating part. A simple model for direct drop generation has been stated and used for spinning disk aerosol generators:

$$D_{0.999} = \frac{1.07}{N}\left(\frac{\sigma_l}{d\rho_l}\right)^{0.5}$$

where

$D_{0.999}$ = droplet size larger than 99.9% of the droplets (essentially, the maximum droplet size)

N = rotational speed, rotations/second

ρ_l = liquid density (kg/m³)

σ_l = liquid surface tension (kg/sec²)

d = disk diameter (m)

For smooth rotating disks, which produce nearly a monodisperse aerosol, this equation describes the expected droplet diameter. Figure 1 presents the estimated maximum droplet diameter

for the fluid studied in these experiments. Because machine tools generally have rotational speeds less than 10,000 rpm, Figure 1 indicates that mist droplets formed by rotary atomization will be smaller than 50–100 μm. In correlations involving liquid flow rates, droplet size increases with liquid flow rate.

In addition to creating large primary droplets, rotary atomization can create smaller droplets. For example, researchers using a laboratory rotary atomizer known as a spinning disk aerosol generator have reported the generation of smaller "satellite droplets." These satellite droplets are an order of magnitude smaller than the primary droplets. These droplets are formed by rupture of the tail connecting the primary droplet to the disk or rotating object. Researchers studying spray atomization also have reported the formation of smaller droplets generated when larger droplets break up.

Spray Atomization

Lefebrve summarized the observed physical phenomena during the breakup of liquids in an air jet.[11] When liquid droplets are accelerated to high air velocities, the difference in velocity between the droplet and the air causes the droplet to deform. As this velocity difference increases, the deformation increases and the droplets ultimately disintegrate into mostly large droplets and smaller satellite droplets. The satellite droplets are formed when these larger droplets are pulled apart. Experimentally, this phenomenon is a function of the velocity difference between the liquid droplet and the air, the droplet size, and the fluid's density, viscosity, and surface tension. The size distribution of oils containing high molecular weight polymers such as polyisobutylene are known to reduce misting and increase the size of oil mist generated by spray atomization.[12] These effects are related experimentally to an increase in the fluid's elongational viscosity, which resists the forces that resist the creation of small droplets.[13]

Droplet Collisions with Solid Objects

Rotating tools and parts to some extent will function as coarse rotary atomizers. The airflow induced by the machining operations causes these larger droplets to hit the walls and release a smaller mist.[14] When a droplet hits a surface, the droplet's kinetic, surface, and potential energies are used to spread the droplet over a much wider surface area.[15,16] The remaining energy is used to create smaller mist particles from the sheet of liquid. This has been termed corona formation. The droplets generated by this process are about 20% of the droplet that strikes the surface. Mist generation by this process is a function of initial droplet diameter, velocity, and the fluid's surface tension, density, and viscosity.

Literature Interpretation

The available information indicates that MWF mist generation is probably complicated and may involve a number of different mechanisms. All of the mechanisms described in the preceding paragraphs involve the fluid's velocity and properties such as density, viscosity, and surface tension. The machining operations affect the fluid's velocity. During machining operations the fluid's velocity varies because of differences in fluid application pressure, the distance through which the fluid falls, the tool's diameter, and rotational speed. In addition, some the mist generation mechanisms involve threshold effects. This suggests that if fluid velocities remain below critical values, mist generation will not occur and control measures are not needed.

To gain some understanding of mist generation during the machining process, an experiment was focused on dissecting the mist generation process. Such an experiment would be done to evaluate whether MWF aerosol generation is due to fluid application velocity, tools speed, or the actual metal cutting process.

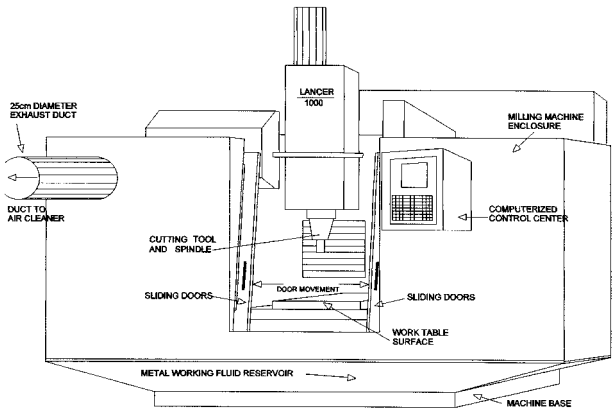

FIGURE 2. Schematic of machining center

EXPERIMENTAL PROCEDURES

Mist generation at a machining center can be thought of as a three-step process with mist generation increasing during each step: (1) The fluid stream starts flowing over a stationary tool; (2) the tool starts rotating and mist generation is increased; and (3) the tool cuts metal. This model is useful in that it allows one to dissect the mist generation process during machining and to obtain some insight as to which processes are important. Two experiments were conducted. A factorial experiment was conducted to evaluate the effect of fluid application velocity, tool revolutions per minute, and metal cutting on mist generation. This experiment was conducted to evaluate which of the three steps mentioned earlier in this paragraph contribute to mist generation. Because tool speed increases the energy available to atomize the MWF, a tool speed experiment was conducted to evaluate the effect of tool diameter and tool speed on mist generation.

Machining Operation

Both experiments were conducted at a Lancer Vertical Machining Center shown schematically in Figure 2. The machining center was almost totally enclosed and 0.25 m^3/sec (540 ft^3/min) of air was exhausted from the enclosure. The exhaust volume was confirmed by tracer gas measurements reported elsewhere.[17] The MWF was a soluble oil (Trimsol, Masterchemical, Perrysburg, Ohio). The fluid's kinematic viscosity was 1.2 centistokes, and its surface tension was 30–33.9 dynes/cm. This fluid was chosen because it was used in about 5–10% of General Motors facilities.

In the machining center, the face milling of a 30.5 by 31-cm rectangular surface of aluminum stock that was 2-cm thick was used to study mist generation. This stock was drilled with a pattern of equally spaced 0.6-cm diameter holes that were 1.2-cm deep. The pattern was 16 columns of 15 equally spaced holes along the 31-cm length of the aluminum. This aluminum stock was clamped to a moveable table. A face mill, with provisions for six carbide teeth, was used to remove 0.04 cm of aluminum during each pass. This face mill had a 10-cm diameter and the mill's teeth were located on a circle 10-cm diameter.

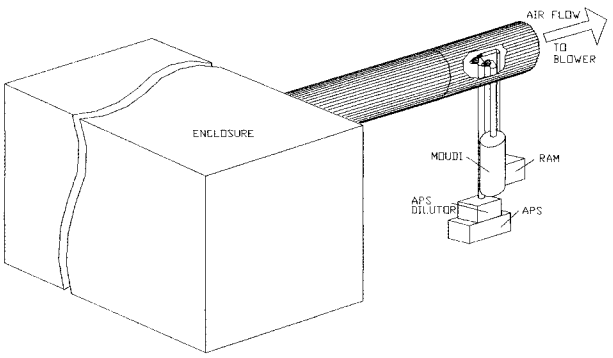

FIGURE 3. Schematic of ventilation and sampling system. The isokinetic sampling probes were located 220 cm from the outlet of the enclosure.

Mist Concentration Measurements

The air cleaner fan drew 0.25 m^3/sec of air into the enclosure through a 25-cm diameter duct, past isoaxial sampling probes, and through a 97% DOP filter before discharging the air back into the facility. As shown in Figure 3, the isoaxial sampling probes were used to transport air samples from the duct to instruments that were used to measure aerosol concentration. The sampling probe nozzles were fabricated from 0.01-cm thick brass shim stock. For each instrument, air entered the probe's nozzle, which expanded to the diameter of the tubing in a distance of 10 cm. After entering the nozzle, the air flowed into a 5-cm horizontal length of a copper tubing, through a copper elbow, and through another straight run of copper tubing. The tubing was common copper pipe, and the elbows for the tubing had a radius of 2R. The diameter of the sampling probes nozzle and the sampling tube for each instrument are given in Table I. The following instruments were used to measure mist concentration.

Aerodynamic Particle Sizer

An aerodynamic particle sizer (APS model 33b, TSI, St. Paul, MN) was used with an APS Diluter (model 3302). In the APS, individual particles are sized based on their transit time between two laser beams. As particles pass through the two laser beams, scattered light is detected by a photo multiplier tube. The time difference between these two events is measured. The diluter was positioned on top of the APS as described in the instrument's operating instructions. A dilution ratio of 20 to 1 was used, and the data were adjusted using the manufacturer's correction for the particle transmission efficiency of the diluter. The APS's detection logic can cause the creation of spurious counts, which have been termed phantom particles. The APS count data was adjusted for phantom particle creation using a procedure that has been described elsewhere.[18] The number concentrations (C_n) were used to compute the mass concentration (C_m) of MWF mist using the channel's diameter (d), and assuming unit density (ρ), with n denoting the number of channels. The following formula was used to compute C_m:

$$C_m = \sum_{i=1}^{n} \left[\frac{n d_i^3 \rho}{6}\right] C_n$$

TABLE I. Inlet Diameters and Velocities for Duct Sampling Probes

Instrument	Sample Tube Diameter (cm)	Inlet Diameter (cm)	Flow Rate (L/min)	Velocity (cm/sec)
APS	1.91	0.46	5	508
RAM	1.27	0.32	2	421
MOUDI	2.54	1.14	30	487

Microorifice Uniform Deposit Impactor

The Microorifice Uniform Deposit Impactor (MOUDI) (Model 100, MSP Corp., Minneapolis, MN)[19] is an eight-stage cascade impactor that was operated at a flow rate of 30 L/min. This impactor is unique in that each stage rotates, allowing the collected material to be uniformly deposited on the filters. The metal removal fluid mist was collected on 37-mm, 5-μm pore size PVC filters (SKC Inc., Eighty-Four, Pa.). The 50% cut diameters for this impactor are 18, 10, 6.2, 3.2, 1.8, 1.0, 0.32, and 0.18 μm. These filters were pre- and postweighed in a temperature- and humidity-controlled environment. The filters were adjusted for the weight change of blank filters. The mass concentrations measured using the MOUDI were adjusted for reported inlet losses.[19] The mass concentration of MWF mist measured by the MOUDI was computed by summing the masses collected on all of the stages and the backup filter and dividing this sum by the sample volume.

Real-Time Aerosol Monitor (RAM)

The RAM-1 (MIE Inc., New Bedford, Mass.) was operated in the 0–2 mg/m^3 range and at a time constant of 2 sec. In the instrument's sensing chamber the RAM measures the quantity of light scattered by the entire cloud. The quantity of scattered light is a function of concentration and the aerosol's optical properties. Thus, this instrument's response is a measure of relative concentration. This instrument was used to look for enclosure leakage and to provide a continuous indication of concentration. The analog output of this instrument was recorded every 10 sec using a data logger (Rustrak Ranger II, Rustrak Instruments, East Greenwich, R.I.).

Temperature and relative humidity were measured with a temperature and relative humidity probe (RR2–252, Rustrak Instruments). The probe was simply inserted into the duct half-way between the air cleaner and the enclosure. The dew point was measured with a dew point meter (Model 911, EG&G, Walther, Mass.). The analog outputs of the temperature and relative humidity probe and the dew point meter were recorded every 10 sec with a multichannel data logger (Ranger II, Rustrak Instruments).

Factorial Design Experiment

The first experiment was conducted to evaluate the effect of the three mist-generating steps mentioned earlier on the mist concentration and size distribution. This experiment was organized as a $2 \times 2 \times 3$ factorial experiment with two extra test conditions. The experimental parameters and their levels were as follows: (1) fluid application velocity, 16.6 or 4.4 m/sec at flow rates of 31.5 and 33 L/min, respectively; (2) tool speed, 1910 or 3800 rpm; and (3) metal cutting conditions, null, 2-mill teeth, or 6-mill teeth. Metal was not cut during the null condition; the spinning face mill with 6-mill teeth was positioned 0.003 to 0.007 cm above the part.

All possible combinations of these variables were tested. For the two extra test conditions, the fluid flowed over a stationary face mill at the two fluid velocities listed above. This experiment involved 14 combinations of test conditions with one replication. Within each replication, the test conditions were run in random

TABLE II. Probability (Probability >F) that Chance Caused Observed Differences in the Dependent Variables

Type of Analysis	Evaluate Whether Independent Variables Affected Shape of Aerosol Distribution		Evaluate Whether Independent Variables Affected Amount of Mist Produced	
	Multivariate Analysis of Variance		Analysis of Variance	
Dependent variable	Mass fraction in Stages 0–3 of the MOUDI	Size distribution APS	MOUDI mass concentration	APS mass concentration
Fluid velocity	0.0047	0.22	0.0001	0.0001
Tool rotational speed	0.0001	0.01	0.0001	0.0001
Interaction of fluid velocity and tool rotational speed	0.0001	0.41	0.0001	0.001

Note: Probabilities less than 0.05 indicate that the independent variable had a significant effect on mist concentration.

order. Every four to six runs, background particulate concentrations were measured for periods of 5–20 min. During background measurements, machining did not occur.

Each experimental run lasted 23 min. During the first 3 min the concentrations were allowed to reach steady state. Preliminary experimental measurements made with an aerosol photometer indicated that mist concentrations required 3 min to reach study state. After 3 min elapsed, data was collected for 20 min.

Tool Speed

In the second experiment, the effect of tool speed on mist generated by rotating tools was evaluated. The machining operation studied was the null condition from the first experiment. The fluid application velocity was 4.5 m/sec. The tools simply rotated above the part being machined. The tools were the 10-cm diameter face mill from the first experiment and a 1.08-cm diameter end mill. The tools rotated 0.003 to 0.007 cm above the aluminum plate. For the 10-cm diameter face mill, the following tool speeds were studied: 3820, 3000, 1910, 1000, 500, and 250 rpm. For the 1.08-cm diameter end mill, the tool speeds were 15,000; 10,000; 7500; 3820; 1910; and 1000 rpm. For each tool diameter the tool speeds were run in random order, twice.

Each experimental run lasted 11 min. During the first 3 min the concentration was allowed to reach study state. After the 3 min had elapsed, the APS was used to measure the concentration and size distribution in the test chamber. Background aerosol concentrations were measured for a period of 5 min after every other experimental run.

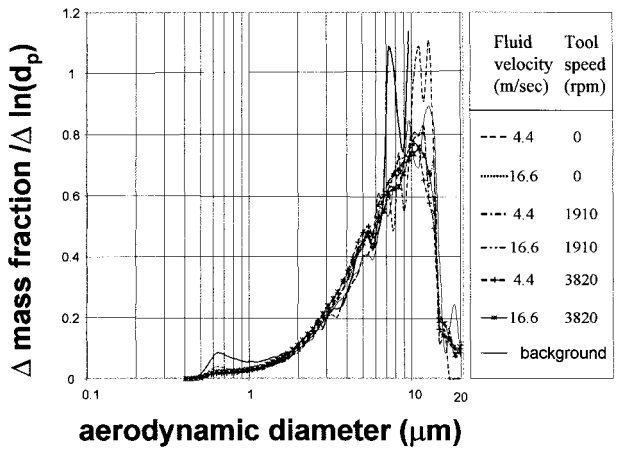

FIGURE 4. Test conditions had little effect on size distributions measured by APS.

RESULTS AND FINDINGS

Temperature and Humidity Measurements

During practically all experimental runs, the dew point and the ambient temperature in the duct were within 1–2°C of each other. Water was observed to leak from the duct. Apparently, the air in the duct was saturated with water.

Factorial Experiment

Size Distribution

The mass fraction of material collected on each impaction stage and in each APS channel was computed. In the statistical analysis of the MOUDI impactor data, the dependent variables in the statistical model were the mass fraction collected on each stage for Stages 0–3. Approximately 80–90% of the mass was collected on these stages. The remaining stages were excluded because of concerns over analytical error. Because these mass fractions are probably dependent on each other, a multivariate analysis was used to evaluate whether test conditions affected the mass fraction in a size range.[20,21] For each variable, a multivariate F-test, Wilk's lambda, was used to evaluate whether chance alone could have caused the observed differences in mass fraction attributed to the settings of the independent variables. This multivariate test considers the correlation between the dependent variables, experimental variability, and the magnitude of the observed differences in the dependent variables.[22] Because a full analysis of the data showed that the variables involving metal cutting did not affect the dependent variables ($p>0.07$), Table II presents results of an analysis conducted to evaluate whether fluid velocity and tool revolutions per minute affected the mass fraction of material collected on Stages 0–3 ($p<0.005$). Before these statistical techniques were applied to the APS data, the mass fraction of material collected in the size ranges approximately corresponding to impactor Stages 1, 2, and 3 of the MOUDI impactor were computed. The third column of Table II presents this analysis. The high probabilities indicate that fluid velocity and metal cutting conditions do not affect the shape of the size distribution measured by the APS. Tool speed did affect ($p=0.01$) the shape of the size distribution.

Figures 4 and 5 graphically present the effect of tool speed and

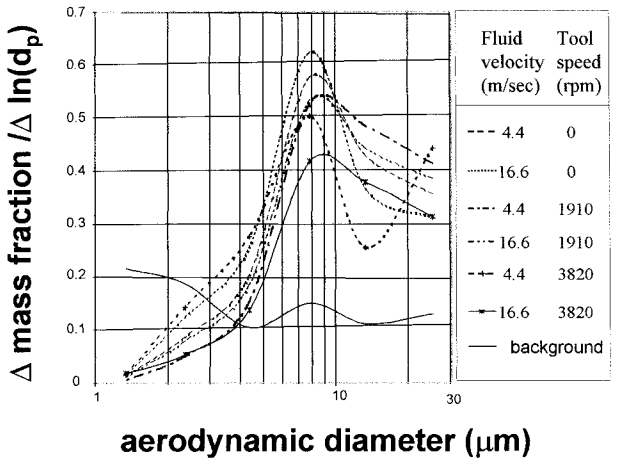

FIGURE 5. High tool speed ppeared to reduce the size of the aerosol measured by the MOUDI. This effect appears to be very pronounced in the 9–18 μm range (MOUDI Stage 1).

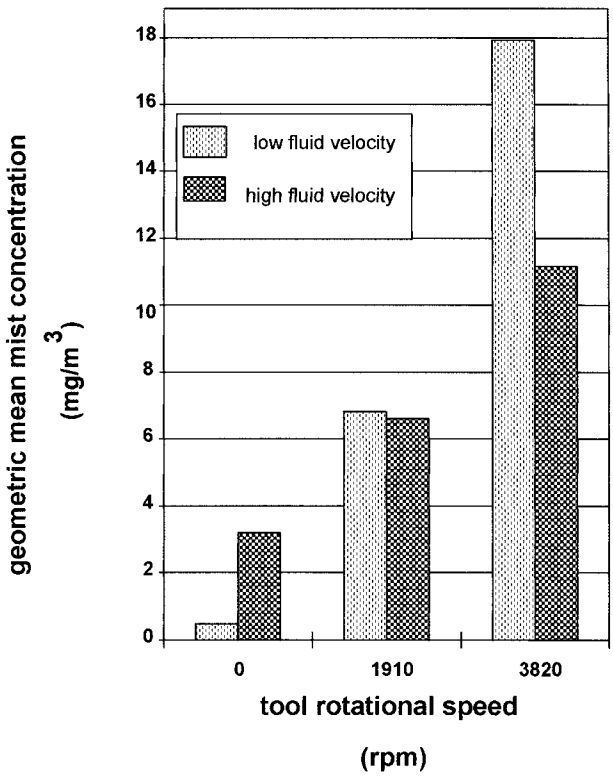

FIGURE 6. Effect of tool speed and fluid application velocity on mist concentrations measured by the MOUDI

fluid application velocity on the shape of the measured size distribution. The ordinate in these figures is the term "Δ mass fraction/Δ $\ln(d_p)$." In this variable, the mass fraction in size range is divided by Δ $\ln(d_p)$. This latter term is literally the logarithm of the ratio of the upper to lower boundaries for each particle size channel. For each impactor stage, these lower and upper boundaries are the 50% cut diameters of the stage and the 50% cut diameter of the preceding stage. In Figure 5 the size distributions measured at a tool speed of 3800 rpm appear to be smaller than the other size distributions measured by the MOUDI. This is consistent with the result of the statistical analysis. This result explains the low probabilities for the tool speed-related effects in Table II. Figure 4 shows that machining conditions had little observable effect on the size distribution measured by the APS. The results of the statistical analysis indicate that the mass fractions measured by the APS were largely unaffected by the independent variable. Only tool speed ($p=0.01$) affected the mass fraction collected in the size ranges. The tool speed effect uncovered by the statistical analysis is not evident in this plot.

Mass Concentration Effects

The SAS general linear models procedure was used to evaluate whether total aerosol concentration measured by the MOUDI and APS was affected by fluid velocity, tool revolutions per minute, metal cutting conditions, and the combinations of these variables.[20] Before data analysis, the logarithms of the concentrations were taken. Because the variances appeared to be nonhomogenous, the analysis was weighted by the reciprocal of the variance for each combination of tool revolutions per minute and fluid velocity. Cutting condition was not considered in weighting the analysis, because variables involving cutting conditions did not affect the measured concentration. Table II presents the results of the analysis when the "cutting" is excluded from the analysis. When cutting was included in the analysis, its effect was insignificant ($p>0.4$). Regardless of which analysis is used, fluid application velocity, tool speed, and the interaction of these two independent variables significantly affected the concentrations measured by the APS and the MOUDI ($p<0.005$).

In Figures 6 and 7 mist generation is plotted as a function of tool revolutions per minute and fluid velocity. In both figures, mist

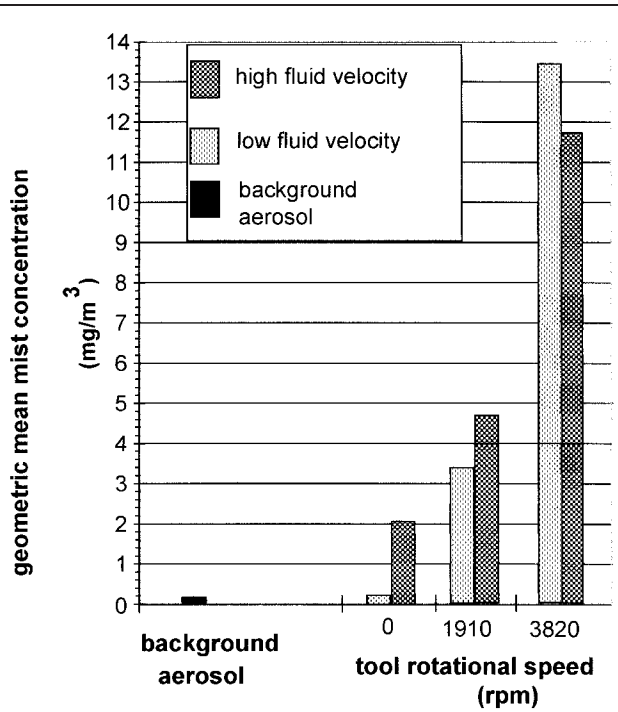

FIGURE 7. Effect of tool speed and fluid application velocity on mist concentrations measured by the APS

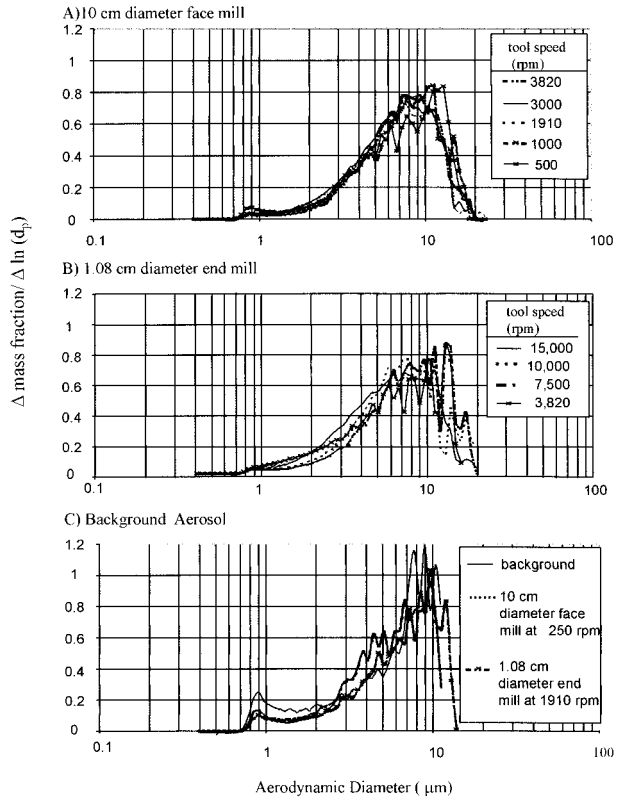

FIGURE 8. Tool speed had a very small effect on the observed size distribution measured by the APS.As tool speed increased, the distributions were shifted slightly to a smaller size. The size distributions measured at the lowest tool speeds were essentially those of background aerosol.

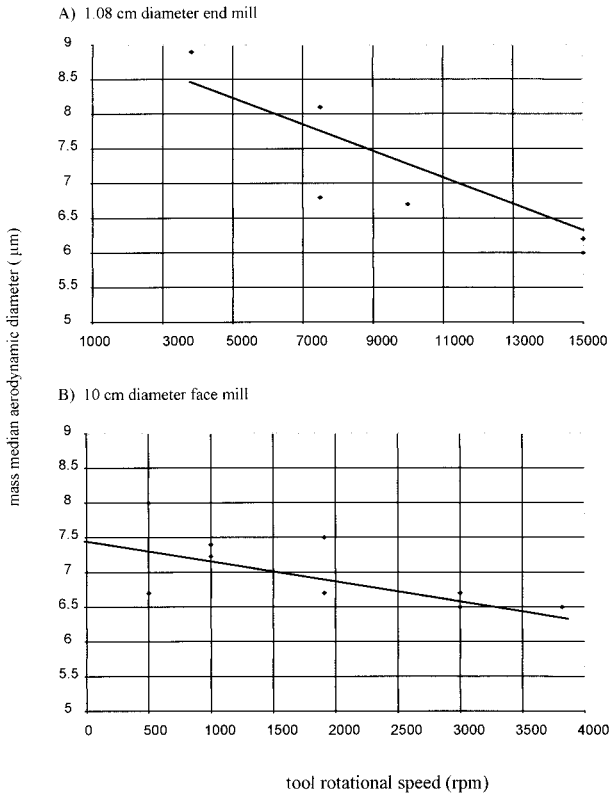

FIGURE 9. Tool speed has a very slight but significant effect on mass median diameter. (For the end mill, p = 0.0079, and for the face mill, p = 0.02.)

concentration increases with increasing tool revolutions per minute and fluid application velocity. For the APS data presented in Figure 7, the effect of fluid velocity decreases with increasing tool speed. At low tool speeds, the higher fluid velocity is associated with higher concentrations. At the high tool speed, this difference appears to be very small. For the MOUDI data presented in Figure 6, fluid application velocity increased mist concentration at the 0 rpm tool speed. At the highest tool speed, the reverse occurred. The reason for this is unclear.

Tool Speed Experiment

Size Distribution

A multivariate analysis of variance (MANOVA) was used to evaluate whether the tool speed and the tool affect the shape of the size distribution.[20] Before conducting the analysis, the mass fraction of material collected in the size ranges approximately corresponding to impactor Stages 1, 2, and 3 of the MOUDI impactor were computed. Then, the mass fraction in the stages was modeled as a function of tool speed and tool diameter. Some of the APS data was excluded from the MANOVA. The mean and standard deviation for the background concentrations were 0.16 and 0.09 mg/m³. When the measured concentration is less than 0.4 mg/m³, the measured aerosol could be largely background aerosol. For a tool diameter of 1.08 cm, tool speeds of 15,000; 10,000; and 7500 rpm and for a tool diameter of 10 cm, tool speeds of 3820, 3000, 1910, 1000, and 500 rpm were included in the analysis of the size distribution. Because of insufficient degrees of freedom, the data from the two tools could not be analyzed separately. Each combination of tool diameter and tool speed was considered a treatment. A MANOVA was conducted to evaluate whether mass fraction of Stages 1, 2, and 3 varied with the treatment. A multivariate F-test, Wilkes's lambda, indicated that treatment had a significant effect on size distribution (prob of > F = 0.0001). This simply indicates that the mass fraction in these stages varies significantly with the treatment.

As shown in Figure 8, tool diameter and tool speed has a very small effect on size distribution. Close examination of the plots indicates that increased tool speed causes the size distribution to shift to a slightly smaller size distribution. In Figure 9 the mass median diameter is plotted as a function of a tool's surface speed for both tool diameters. The tool surface speed is the product of the tool's circumference and the tool's rotational frequency. In Figure 9, a 500–800% change in tool surface speed is required to reduce the mass median diameter by 12–25%. Apparently, particle size changes vary slowly with tool surface speed.

Concentration Effects

The effect of tool speed on mass concentration is presented in Figure 10 for measured concentrations greater than 0.2 mg/m³. Regression analysis obtained from SAS results in Table III showed that tool surface speed can dramatically increase mist concentration.[20] Based on regression analysis, mass concentration is proportional to the 2 and 3.5 power of tool surface speed for tool diameters of 1.08 and 10 cm. Given the same surface velocity, the smaller tool is more effective at creating mist. The smaller tool is

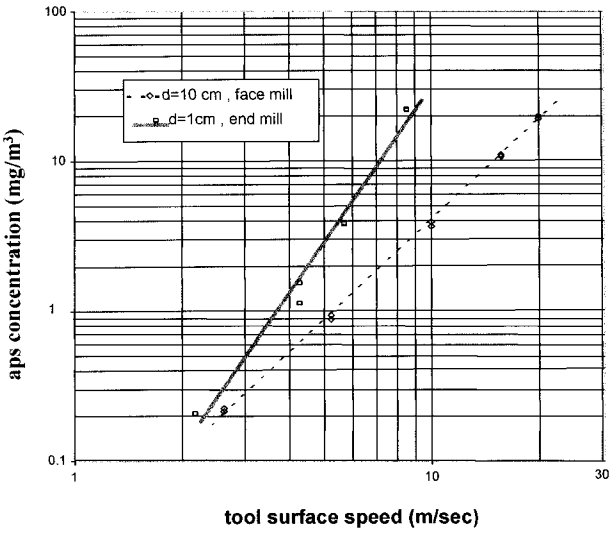

FIGURE 10. Tool speed and tool diameter affect the amount of mist generated. The effect of tool speed appears to vary with diameter. Concentrations lower than 0.2 mg/m³ were not plotted or shown because these concentrations reflect background aerosol.

subjecting the fluid to a higher centrifugal acceleration. For uniform circular motion, centrifugal acceleration is the square of velocity divided by the radius.[23]

DISCUSSION

These two experiments showed that mist generation is a function of fluid motion. The amount of mist generated increases with fluid application pressure and tool speed. In the factorial experiment, the mist concentration increased with increasing tool speed and fluid application pressure, which are both measures of fluid velocity. The actual metal removal did not significantly affect the amount of mist generated. During the study of tool speed, mist concentration was proportional to the 2–3.5 power of tool surface speed. Increasing tool speed can cause a very noticeable increase in mist concentration. Thus, when tool speeds are increased, industrial hygienists need to review the mist control measures in place. These findings are consistent with the industrial observation that mist generation can be minimized by minimizing fluid delivery pressures and flow rates.[24]

The experimental parameters studied had little effect on the measured aerosol size distribution. Although the statistical analysis used for the factorial experiment indicated significant changes in the measured size distribution, the results presented in Figures 4 and 5 indicate that tool speed and fluid application pressure have only a slight effect on mist size. In Figure 9 a 500–800% increase in tool speed causes a 12–25% decrease in particle size. This situation suggests that tool speeds can be altered without causing the generation of an excessive mass of smaller particles that could easily penetrate an air cleaner.

Based on the particle size results presented in Figures 4 and 5, 99% of the aerosol mass is in particles larger than 1 μm. This suggests that air cleaners that remove particles larger than 1 μm will control practically all of the worker's exposure to metal removal fluids. This result is consistent with results reported in a study conducted in an actual plant.[5]

In this study, the fluid evaporation and condensation did not lead to the creation of particles smaller than 1 μm. In another study of aerosol formation at a lathe, a significant fraction of the aerosol formed was smaller than 1 μm and was thought to be formed by evaporation and condensation.[25] In the latter study, the fluid application rates were below 1 mL/min. In the present study, the fluid application rate was approximately 31 L/min. The difference in the findings of the two studies can be explained by the difference in the fluid application rates. At low fluid application rates the heat of production is removed by evaporation. At high fluid application rates, the fluid absorbs the heat of production without a noticeable rise in temperature or fluid evaporation.

Because this study was conducted with a commercially available machining center and a commonly used MWF, the study findings are applicable to many machining operations. Extrapolation of the results presented here to other conditions is more difficult. Perhaps, mathematical models of mist generation by MWF could be devised that would incorporate many of the possible mist generation mechanisms. Such a model could be either theoretical or semitheoretical based on dimensional analysis and similitude.[26,27] These models could be used to guide experimentation and to extrapolate and perform scale-up calculations to estimate mist generation rates for conditions that have not been studied experimentally.

TABLE III. Regression Analysis Results for Relationship Between Tool Speed and Mist Generation

Term	Tool Diameter = 10 cm	Tool Diameter = 1 cm
Slope	2.2 ± 0.05	3.4 ± 0.4
Intercept	−3.6 ± 0.12	−4.57 ± 0.8
Geometric standard deviation from root mean	1.07	1.3
Probability of a significant deviation from a normal distribution of residuals	0.60	0.26

CONCLUSIONS

The machining operations studied did not greatly affect the size distribution of the aerosol. Based on the particle size results, air cleaners that are very efficient for particles larger than 1 μm will control practically all of the worker's exposure to metal removal fluids. However, mist generation increased dramatically with tool surface speed.

When tool speeds are increased, industrial hygienists need to review mist control methods. Increased fluid velocities may cause an increase in the amount of mist generated. In addition, the amount of mechanically induced airflow may increase, causing mist-laden air to leak from enclosures. Because both phenomena can cause increased mist exposures, exposure monitoring needs to be performed when tool speeds are increased. Since tool speeds are increased to improve productivity, restrictions on tool speeds are probably an unacceptable control option. Realistic mist control options will probably involve minimizing mist leakage from enclosures, ventilating the enclosure, and the selection of appropriate air cleaners.

REFERENCES

1. **Kennedy, S.M., I.A. Greaves, D. Kriebel, E.A. Eisen, T.J. Smith, and S.R. Woskie:** Acute pulmonary responses among automobile workers exposure to aerosols of machining fluids. *Am. J. Ind. Med 15*: 627–641 (1989).
2. **Hendy, M.S., B.E. Beattie, and P.S. Burge:** Occupational asthma due to an emulsified oil mist. *Br. J. Ind. Med. 42*:51–54 (1985).
3. **Eisen, E.A.:** Case-control studies of five digestive concerns and exposure to metalworking fluids. In *Symposium Proceedings: The Industrial Metalworking Environment: Assessment and Control.* Detroit, MI: American Automobile Manufacturers Association. 1996. pp. 25–28.
4. **National Institute for Occupational Safety and Health (NIOSH):** *Criteria for a Recommended Standard—Occupational Exposure to Metal Working Fluids* (DHHS [NIOSH] pub. no. 98–102). Cincinnati, OH: NIOSH, 1997.
5. **Yacher, J.M., W.A. Heitbrink, G.E. Burroughs, and M.A. Sullivan:** Case study: mist control following installation of air cleaners on machining centers. In *Proceedings of Metal Working Fluids Symposium II—The Industrial Metal Working Environment: Assessment and Control of Metal Removal Fluids.* Detroit, MI: American Automobile Manufacturers Association. 1997.
6. **Raynor, P.C., S. Cooper, and D. Leith:** Evaporation of polydisperse multicomponent oil droplets. In *Symposium Proceedings—The Industrial Metal Working Environment—Assessment and Control, November 13–16, Dearborn, Michigan*. Washington, DC: American Automobile Dealers Association, 1996.
7. **Hoyt, J.W., J.J. Taylor, and C.D. Runge:** The structure of jets of water and polymer solutions in air. *J. Fluid Mech. 63*:634–640 (1974).
8. **Bhunia, S.K., and J.H. Lienhard:** Splattering during turbulent liquid jet impingement on solid targets. *Trans. ASME J. Fluids Engin. 116*:338–344 (1994).
9. **Bhunia, S.K., and J.H. Lienhard:** Surface disturbance evolution of turbulent liquid jets. *Trans. ASME J. Fluids Engin. 116*:721–727 (1994).
10. **Childers, J.C.:** The chemistry of metal working fluids. In *Metal Working Fluids,* J.P. Byers (ed.), New York: Marcel Dekker, 1994.
11. **Lefebvre, A.H.:** *Atomization and Sprays.* New York: Hemisphere Publishing, 1989. pp. 421.
12. **Gulari, E., C.W. Manke, J. Smolinski, R.S. Maran, and L. Toth**: Polymer additives as mist suppressants in metalworking fluids: Laboratory and plant studies. In *Symposium Proceedings—The Industrial Metal Working Environment—Assessment and Control, November 13–16, Dearborn, Michigan*. Washington, DC: American Automobile Dealers Association, 1995. pp. 294–300.
13. **Smolinski, J., E. Gulare, and C.W. Manke:** Atomization of dilute polyisobutylene/mineral oil solutions. *Am. Ind. Hyg. Assoc. J. 42*: 1201–1211 (1996).
14. **Earnest, G.S., W.A. Heitbrink, R.L. Mickelsen, and J.B. D'Arcy:** Evaluation of leakage from a metal machining center using tracer gas. In *Proceedings of Metal Working Fluids Symposium II, The Industrial Metal Working Environment: Assessment and Control of Metal Removal Fluids, September 15–18, 1997.* Detroit, MI: American Automobile Manufacturers Association. 1997.
15. **Mundo, C., M. Sommerfield, and C. Tropea:** Droplet–wall collisions: Experimental studies of the deformation and breakup process. *Int. J. Multiphase Flow 21*:151–173 (1995).
16. **Rein, M.:** Phenomena of liquid impact on solid and liquid surfaces. *Fluid Dynam. Res. 12*:61–93 (1993).
17. **Earnest, G.S., W.A. Heitbrink, R.L. Mickelsen, K.R. Mead, and J.B. D'Arcy:** Leakage from a metal machining center—a case study. In *Proceedings of Metal Working Fluids Symposium II—The Industrial Metal Working Environment: Assessment and Control of Metal Removal Fluids.* Detroit, MI: American Automobile Manufacturers Association, 1997.
18. **Heitbrink, W.A., and P.A. Baron:** An approach to evaluating and correcting aerodynamic particle size measurements for phantom particle count creation. *Am. Ind. Hyg. Assoc. J. 53*:427–431 (1992).
19. **Marple, V.A., K.L. Rubow, and S.M. Behm:** A microorifice uniform deposit impactor (moudi): description, calibration, and use. In *Micro-Orifice Uniform Deposit Impactor Instruction Manual.* Minneapolis, MN: MSP Corp., 1992. Appendix A.
20. **SAS Institute Inc.:** The GLM procedure. In *SAS/STAT User's Guide*. Cary, NC: SAS Institute Inc., 1988.
21. **Bernstein, I.H.:** *Applied Multivariate Analysis.* New York: Springer-Verlag, 1985.
22. **Morrison, D.F.:** *Multivariate Statistical Methods.* New York: McGraw Hill, 1967. p. 338.
23. **Serway, R.A.:** *Physics for Scientists and Engineers/with Modern Physics.* New York: Saunders College Publishing, 1983. p. 193.
24. **American National Standards Institute:** *ANSI Technical Report for Machine Tools—Mist Control Considerations for the Design and Use of Machine Tools Using Metal Working Fluids* (ANSI B11 TR2–1997). McLean, VA: Association for Manufacturing Technology, 1997.
25. **Thornburg, J., and D. Leith:** Mist generation rate and size distribution during machining. *Proceedings of Metal Working Fluids Symposium II—The Industrial Metal Working Environment: Assessment and Control of Metal Removal Fluids.* Detroit, MI: American Automobile Manufacturers Association, 1997.
26. **McCabe, W.L., and J.C. Smith:** *Unit Operations of Chemical Engineering.* New York: McGraw Hill, 1967. pp. 18–22.
27. **Fox, R.W., and A.T. McDonald:** *Introduction to Fluid Mechanics.* New York: Wiley, 1985. pp. 295–330.